NACA

RESEARCH MEMORANDUM

for the

Air Materiel Command, U. S. Air Force

WIND-TUNNEL INVESTIGATION OF A 0.6-SCALE MODEL OF HUGHES MX-904 TAIL SURFACE AT SUPERSONIC SPEEDS

TAIL ATTACHED TO A SEGMENT OF THE FORESHORTENED BODY

By D. William Conner and Lawrence D. Guy

Langley Aeronautical Laboratory
Langley Air Force Base, Va.

NATIONAL ADVISORY COMMITTEE FOR AERONAUTICS

WASHINGTON

MAY 1950

NATIONAL ADVISORY COMMITTEE FOR AERONAUTICS

RESEARCH MEMORANDUM

for the

Air Materiel Command, U. S. Air Force

WIND-TUNNEL INVESTIGATION OF A 0.6-SCALE MODEL OF HUGHES MX-904 TAIL SURFACE AT SUPERSONIC SPEEDS

TAIL ATTACHED TO A SEGMENT OF THE FORESHORTENED BODY

By D. William Conner and Lawrence D. Guy

SUMMARY

An investigation has been made of a partial-span model of the tail surface designed for use on the Hughes Falcon (MX-904) missile to determine the aerodynamic characteristics of the tail and elevator including elevator hinge moment. Data obtained at Mach numbers of 1.62 and 1.96 in the Langley 9- by 12-inch supersonic blowdown tunnel are presented for the condition where the tail was attached to a segment of the foreshortened body.

INTRODUCTION

At the request of the Air Materiel Command, U. S. Air Force, an investigation is being made in the Langley 9- by 12-inch supersonic blowdown tunnel of a partial-span model of the tail surface designed for use on the Hughes Falcon (MX-904) missile. A model of the complete missile has been investigated in the Langley 9-inch supersonic wind tunnel, as reported in reference 1. The purpose of the present investigation is to determine, at supersonic speeds, the characteristics of the tail and elevator, including the elevator hinge moment, for a range of elevator deflections and tail angles of attack. Data at Mach numbers of 1.62 and 1.96 are presented only for the condition when the tail was attached to a segment of the foreshortened fuselage. Reynolds number based on body

diameter was about 2×10^6. Additional tests are now underway to investigate the breakdown of loading between the tail and fuselage as well as to determine the effects of fuselage segment size on the results. In order to expedite publication of these data, no analysis of the results is given.

SYMBOLS

All data are referred to the wind axes.

C_L	lift coefficient $\left(\frac{\text{Lift}}{qS}\right)$
C_D	drag coefficient $\left(\frac{\text{Drag}}{qS}\right)$
C_m	pitching-moment coefficient $\left(\frac{m}{qSd}\right)$
$C_{l_{gross}}$	gross rolling-moment coefficient $\left(\frac{L}{qSd}\right)$
$C_{n_{gross}}$	gross yawing-moment coefficient $\left(\frac{N}{qSd}\right)$
m	pitching moment of partial-span model about reference lateral axis (see fig. 1)
L	rolling moment of partial-span model about reference longitudinal axis (see fig. 1)
N	yawing moment of partial-span model about reference vertical axis
C_h	elevator hinge-moment coefficient $\left(\frac{\text{Elevator hinge moment}}{2M_aq}\right)$
α	angle of attack, degrees
δ	elevator deflection with respect to tail chord line, degrees
B_2	designation of body configuration
B_2T	designation of body-tail configuration

[redacted]

q	dynamic pressure
S	half cross-sectional area of complete body (5.79 sq in.)
d	diameter of complete body (3.84 in.)
M_a	moment of the area of elevator aft of hinge line about hinge axis (1.34 cu in.)
M	Mach number

MODEL

Geometric details of the model are presented in figure 1 and photographs are shown in figure 2. The model, furnished by the Hughes Aircraft Company, consisted of a 0.6-scale version of one tail surface designed for the Falcon (MX-904) missile combined with a segment of the body.

The tail surface, fabricated from stainless steel, had a pivoted elevator which was fixed in position by pinning it to a restraining arm which extended to the rear of the fuselage. The elevator pivot consisted of a small pin near the outboard end and a shaft extending inside the fuselage through a ball bearing. Four strain gages mounted on the restraining arm permitted measurement of the elevator hinge moment with complete compensation for temperature effects. Friction of the system appeared to be negligible.

For these tests the tail surface was attached to a segment of the foreshortened body, and loads were measured on the combination. Basic tail-off tests were made for the plain body. A small gap existed between the fuselage and the tunnel floor. An insulated charged plate attached to the fuselage permitted an indication of model fouling.

APPARATUS

The tests were conducted in the Langley 9- by 12-inch supersonic blowdown tunnel, which is of the nonreturn type and utilizes the compressed air of the Langley 19-foot pressure tunnel. The absolute stagnation pressure of the air ranged from 2 to $2\frac{1}{3}$ atmospheres. In order to insure condensation-free flow in the test section, the air is conditioned before entering the settling chamber by being passed through a silica gel dryer and then through 12 banks of finned electrical heaters. Three

turbulence-damping screens are located in the settling chamber. Various test section Mach numbers are provided by different nozzle blocks which, by means of quick-acting pneumatic clamps, can be interchanged in a few minutes. Both the $M = 1.62$ nozzle and the air-conditioning equipment have but recently been put into operation, and evaluation of the flow conditions in the tunnel has not been completed. Preliminary calibration of the tunnel indicates satisfactory flow conditions in the test section for both Mach numbers except for a disturbance which appears in schlieren photographs at $M = 1.62$ with the model removed. This disturbance crosses the plane of symmetry ($\alpha = 0^\circ$) about 4.2 inches behind the pitch axis. The elevator might be operating in disturbed flow at negative values of angle of attack or of elevator setting. The following table lists the maximum recorded deviations in calibration measurements taken at approximately 150 positions in the test-section region; properties of the conditioned air are also included:

Variable \ Average Mach number	1.615	1.955
Deviation in Mach number	±0.015	±0.020
Deviation in ratio of static pressure to stagnation pressure	±1.5 percent	±2.0 percent
Deviation in stream angle	±.2°	±.2°
Maximum dewpoint temperature	−10° F	−25° F
Minimum stagnation temperature	140° F	165° F

It should be pointed out that the average operating conditions are much better than the extreme conditions given in the preceding table.

In the arrangement used, the partial-span model was cantilevered from a strain-gage balance which mounts flush with the tunnel wall and rotates with the model through the angle-of-attack range. Simultaneous photographic recording is made of the stagnation pressure, stagnation temperature, balance angle of attack, and model air loads. The balance data are measured with respect to the electrical axes of the balance and are then rotated and transferred by conventional computing methods to allow presentation with respect to the wind axes.

TESTS

For each test the elevator deflection was fixed at a given angle and the model was rotated through an angle-of-attack range. The angle-of-attack range was limited principally by model fouling caused by balance deflection although maximum balance load ratings were sometimes reached. The elevator deflection was determined under no load by measuring the trailing-edge displacement with a depth micrometer both before and after each run. Control deflection was limited to extreme values of about $\pm 15^{\circ}$ by interference between the positioning sector and the fuselage. The hinge-moment measuring apparatus was calibrated before and after these tests and the two calibrations agreed. For the elevator calibration, the model was installed on the balance in the same attitude as was used in testing and loads were applied at right angles to the mid-span point of the trailing edge by means of weights acting through a flexure plate pivot. The dead load of the calibration fixture was counterbalanced. During the calibration, measurements were obtained of the change in control deflection caused by hinge moment. This correction was applied to the data.

The body was positioned parallel with the edge of the tunnel floor (nozzle block removed) with an accuracy of about 0.01°. No measurement was made of possible incidence between body and tail surface.

For the body-alone tests, the body center line was displaced 0.0625 inch from the balance axis. Since side force was not measured, the rolling-moment data could not be shifted to the proper axis. For the body-plus-tail configuration, the axes were alined.

During the course of each test the dynamic pressure and Reynolds number decreased about 5 percent because of the decreasing pressure of the inlet air. For the range of test conditions the values of dynamic pressure as measured in pounds per square inch were about 11.2 (± 1.0) and 10.5 (± 1.0) for $M = 1.62$ and $M = 1.96$, respectively; the corresponding values of Reynolds number were $2{,}100{,}000 \pm 200{,}000$ and $1{,}900{,}000 \pm 200{,}000$ based on the full body diameter. (The body diameter was about equal to the mean aerodynamic chord of the tail surface.

PRECISION OF DATA

As indicated previously, preliminary calibration has shown the stream to be uniform within a maximum variation of Mach number of ± 1 percent.

No tare corrections have been applied to any of the data presented. Some loads could possibly be carried on the elevator-positioning sector located in the rear of the bluff body. All of the force components were measured by means of self-balancing potentiometers. The data have been corrected for all interaction effects between the various components except for an error in chord force introduced by side force amounting to −0.02 pound chord force per pound side force. Although side force was not measured, it probably was of sizable magnitude as evidenced by the large measured yawing moments of the partial fuselage. An estimate of the maximum probable errors in the measurements is given in the following table:

Component	As measured	Coefficient
Lift	±1 lb	±0.02
Drag	0.2 lb	.004
Pitching moment	1 in-lb	.005
Rolling moment	4 in-lb	.01
Yawing moment	4 in-lb	.01
Hinge moment	0.1 in-lb	.005

Angles of attack were determined by static calibration of the balance linkage system with a correction applied for twist caused by model pitching moment. The accuracy is believed to be within ±0.03°. Elevator deflection angles have been corrected for twist caused by hinge moment and are believed to be accurate to within ±0.1°.

PRESENTATION OF DATA

In an effort to present the data in a readily usable form, consideration was given to the twisting effects of air loads on elevator deflection angle and angle of attack. By presetting the angle-of-attack mechanism to approximately account for balance twist caused by elevator deflections, it was possible to obtain data throughout the range of elevator settings at essentially constant values of angle of attack. The basic aerodynamic data are plotted in figures 3 and 4 against elevator deflection for average constant values of angle of attack at the two test Mach numbers. Exact values of both α and δ, given in tables I and II for all test points,

were considered in fairing the curves. Cross plots of these data with angle of attack as the variable are presented in figures 5 and 6 along with the measured basic body-alone data.

It should be pointed out that lift, drag, and pitching-moment data apply to a full-span tail condition with both elevators deflected. The increments obtained in gross rolling moment and gross yawing moment caused by elevator deflection, however, apply to just one control deflected on a complete model.

Decided changes in slope occur in some of the curves for $M = 1.62$ at negative angles of attack. These changes are believed to result not from some peculiarity of the model but from a disturbance in the test section as pointed out in the section on apparatus. The remainder of the data are considered to be reliable within the limits of the test technique employed. Considerable scatter was noticed in the yawing-moment data. A nonlinear variation of gross rolling moment with elevator deflection occurred for both Mach numbers at positive angles of attack and is probably characteristic of this arrangement. In evaluating the data, consideration should be given to the body upwash conditions which would differ from those of the Falcon missile, since only a segment of the circular body cross section was used and since the body extended only a short distance ahead of the tail.

Langley Aeronautical Laboratory
National Advisory Committee for Aeronautics
Langley Air Force Base, Va.

James G. McHugh
for
D. William Conner
Aeronautical Research Scientist

Lawrence D. Guy
Aeronautical Research Scientist

Approved: Mark R. Nichols
for Clinton H. Dearborn
Chief of Full-Scale Research Division

DLMcC

REFERENCE

1. Rainey, Robert W.: Langley 9-Inch Supersonic Tunnel Tests of a Model of the Hughes Aircraft Company MX-904 Missile. Presentation of Three-Component Data Results. NACA RM SL9L30, 1949.

TABLE I.- VALUES OF ANGLE OF ATTACK AND ELEVATOR DEFLECTION FOR DATA PRESENTED IN FIGURE 3. M = 1.62

Average α, deg \ Average δ, deg		-3.5	-3.5 Check	-1.5	-1.5 Check	0.5	0.5 Check	2.0	2.0 Check
-14.2	α								
	δ								
-11.9	α								
	δ								
-9.85	α					-9.72		-9.80	
	δ					.960		2.78	
-7.8	α	-7.65		-7.71		-7.74		-7.79	
	δ	-2.84		-1.03		.83		2.61	
-5.9	α	-5.65		-5.74		-5.78		-5.84	
	δ	-2.94		-1.14		.66		2.44	
-3.9	α	-3.71		-3.79		-3.83		-3.89	
	δ	-3.06		-1.26		.54		2.32	
-1.9	α	-1.75		-1.82		-1.87		-1.94	
	δ	-3.16		-1.35		.45		2.23	
0	α	.21	0.21	.14	0.14	.08	0.05	.02	0.02
	δ	-3.26	-3.26	-1.43	-1.42	.37	.37	2.16	2.16
2.0	α	2.16	2.16	2.10	2.10	2.04	2.02	1.97	1.98
	δ	-3.35	-3.35	-1.50	-1.49	.29	.29	2.06	2.07
4.0	α	4.12	4.12	4.05	4.05	3.99	3.97	3.91	3.90
	δ	-3.43	-3.42	-1.57	-1.57	.20	.19	1.95	1.97
5.9	α	6.04	6.05	5.99	5.97	5.92	5.92	5.83	5.83
	δ	-3.53	-3.53	-1.68	-1.68	.08	.07	1.82	1.84
7.8	α	7.97	7.97	7.91	7.91	7.83	7.81	7.76	
	δ	-3.67	-3.67	-1.81	-1.81	.06	-.07	1.69	
9.8	α		9.88	9.84	9.81	9.75			
	δ		-3.82	-1.94	-1.95	.21			

[redacted]

TABLE I.- VALUES OF ANGLE OF ATTACK AND ELEVATOR DEFLECTION FOR DATA PRESENTED IN FIGURE 3. M = 1.62 - Concluded

Average α, deg		Average δ, deg: 4.0	4.0 Check	6.0	8.5	8.5 Check	14.5	14.5 Check
−14.2	α							−14.22
	δ							15.20
−11.9	α	−11.85		−11.90				−12.22
	δ	4.78		6.62				15.03
−9.85	α	−9.83		−9.93	−9.80	−9.99	−9.84	−10.23
	δ	4.63		6.45	9.12	9.05	14.80	14.84
−7.8	α	−7.86		−7.82	−7.77	−8.03	−7.82	−8.27
	δ	4.44		6.28	8.87	8.86	14.60	14.64
−5.9	α	−5.91	−5.93	−5.99	−5.84	−6.09	−5.86	−6.31
	δ	4.28	4.29	6.13	8.71	8.69	14.44	14.58
−3.9	α	−3.97	−3.96	−4.02	−4.11	−4.14	−3.95	
	δ	4.18	4.17	6.04	8.61	8.58	14.35	
−1.9	α	−2.01	−2.00	−2.06	−1.91	−2.16	−1.94	
	δ	4.10	4.10	5.96	8.53	8.51	14.28	
0	α	−.05	−.04	−.20	−.02		−.05	
	δ	4.01	4.01	5.88	8.43		14.19	
2.0	α	1.91	1.91	1.86	2.01			
	δ	3.92	3.92	5.78	8.35			
4.0	α	3.85	3.86	3.80	4.00			
	δ	3.82	3.82	5.68	8.25			
5.9	α	5.78	5.78					
	δ	3.71	3.71					
7.8	α							
	δ							
9.8	α							
	δ							

NACA

[redacted]

TABLE II.- VALUES OF ANGLE OF ATTACK AND ELEVATOR DEFLECTION

FOR DATA PRESENTED IN FIGURE 4. M = 1.96

Average δ, deg / Average α, deg		-14	-9	-3.5	-3.5 Check	-1.5	-1.5 Check	0	0 Check
-16.0	α		-15.99						
	δ		-8.24						
-14.0	α		-13.91			-13.96		-14.02	
	δ		-8.29			-.91		.96	
-11.95	α		-11.84	-11.88		-11.88		-11.91	
	δ		-8.35	-2.89		-.97		.90	
-9.9	α		-9.78	-9.79		-9.84		-9.86	
	δ		-8.41	-2.95		-1.03		.83	
-7.85	α		-7.78	-7.78		-7.82		-7.84	
	δ		-8.48	-3.01		-1.12		.73	
-5.85	α		-5.78	-5.78		-5.82		-5.84	
	δ		-8.56	-3.05		-1.22		.63	
-3.9	α		-3.80	-3.80		-3.84		-3.87	
	δ		-8.63	-3.21		-1.32		.53	
-1.95	α		-1.82	-1.82		-1.86		-1.89	
	δ		-8.71	-3.29		-1.40		.44	
.05	α	0.28	.15	.16	0.16	.12	0.12	.09	0.09
	δ	-13.80	-8.77	-3.37	-3.38	-1.45	-1.45	.37	.37
2.05	α	2.27	2.14	2.14	2.12	2.10	2.10	2.07	2.07
	δ	-13.89	-8.84	-3.44	3.44	-1.53	-1.53	.30	.30
4.0	α	4.22	4.11	4.11	4.11	4.07	4.08	4.04	4.02
	δ	-13.95	-8.91	-3.51	-3.51	-1.61	-1.60	.22	.22
6.0	α	6.18	6.07	6.09	6.07	6.03	6.03	6.00	5.99
	δ	-14.05	-8.99	-3.60	-3.59	-1.69	-1.69	.13	.13
8.0	α	8.13	8.02	8.03	8.01	7.99	7.99	7.95	7.95
	δ	-14.16	-9.10	-3.69	-3.69	-1.78	-1.78	.04	.04
9.95	α	10.07	9.97		9.99	9.94	9.92	9.90	9.89
	δ	-14.28	-9.22		-3.77	-1.87	-1.86	-.06	-.05
11.9	α	12.02	11.65		11.96			11.87	11.87
	δ	-14.38	-9.32		-3.85			-.14	-.13
13.9	α	13.99	13.92					13.85	13.85
	δ	-14.48	-9.43					-.21	-.20
15.8	α		15.90						
	δ		-9.51						

NACA

[redacted]

TABLE II.- VALUES OF ANGLE OF ATTACK AND ELEVATOR DEFLECTION

FOR DATA PRESENTED IN FIGURE 4. M = 1.96 – Concluded

Average δ, deg / Average α, deg		2.0	2.0 Check	4	4 Check	6	8.5	8.5 Check	14.5	14.5 Check
−16.0	α									
	δ									
−14.0	α			−14.05						−14.31
	δ			4.76						15.26
−11.95	α	−11.92		−11.98						−12.25
	δ	2.81		4.69						15.16
−9.9	α	−9.89		−9.93		−9.99	−9.92	−10.06	−9.92	−10.21
	δ	2.71		4.59		6.47	9.22	9.14	15.06	15.05
−7.85	α	−7.88		−7.92		−7.96	−7.81	−8.01	−7.85	−8.21
	δ	2.59		4.48		6.37	9.09	9.02	14.93	14.94
−5.85	α	−5.88		−5.93		−5.96	−5.84	−6.02	−5.84	−6.22
	δ	2.47		4.37		6.27	8.96	8.91	14.80	14.83
−3.9	α	−3.91		−3.95	−3.95	−4.01	−3.9	−4.05	−3.91	−4.24
	δ	2.36		4.27	4.27	6.17	8.85	8.82	14.71	14.74
−1.95	α	−1.93		−1.97	−1.97	−2.02	−1.88	−2.07	−1.91	−2.26
	δ	2.28		4.19	4.20	6.10	8.77	8.74	14.64	14.67
.05	α	.04	0.05	.01	.01	−.05	.02	−.19	.02	
	δ	2.20	2.21	4.12	4.12	6.03	8.70	8.64	14.55	
2.05	α	2.02	2.01	1.99	1.98	1.85	2.03	1.79	1.97	
	δ	2.13	2.14	4.04	4.04	5.96	8.62	8.58	14.48	
4.0	α	3.99	4.00	3.95	3.95	3.82	4.02	3.75	3.94	
	δ	2.04	2.05	3.95	3.95	5.89	8.53	8.50	14.39	
6.0	α	5.95	5.93	5.91	5.88		5.98		5.83	
	δ	1.94	1.96	3.86	3.86		8.45		14.30	
8.0	α	7.90	7.88	7.86	7.86		7.99			
	δ	1.83	1.86	3.76	3.77		8.36			
9.95	α	9.85	9.87	9.80	9.80		9.94			
	δ	1.74	1.77	3.68	3.68		8.29			
11.9	α		11.88							
	δ		1.69							
13.9	α		13.78							
	δ		1.64							
15.8	α		15.78							
	δ		1.64							

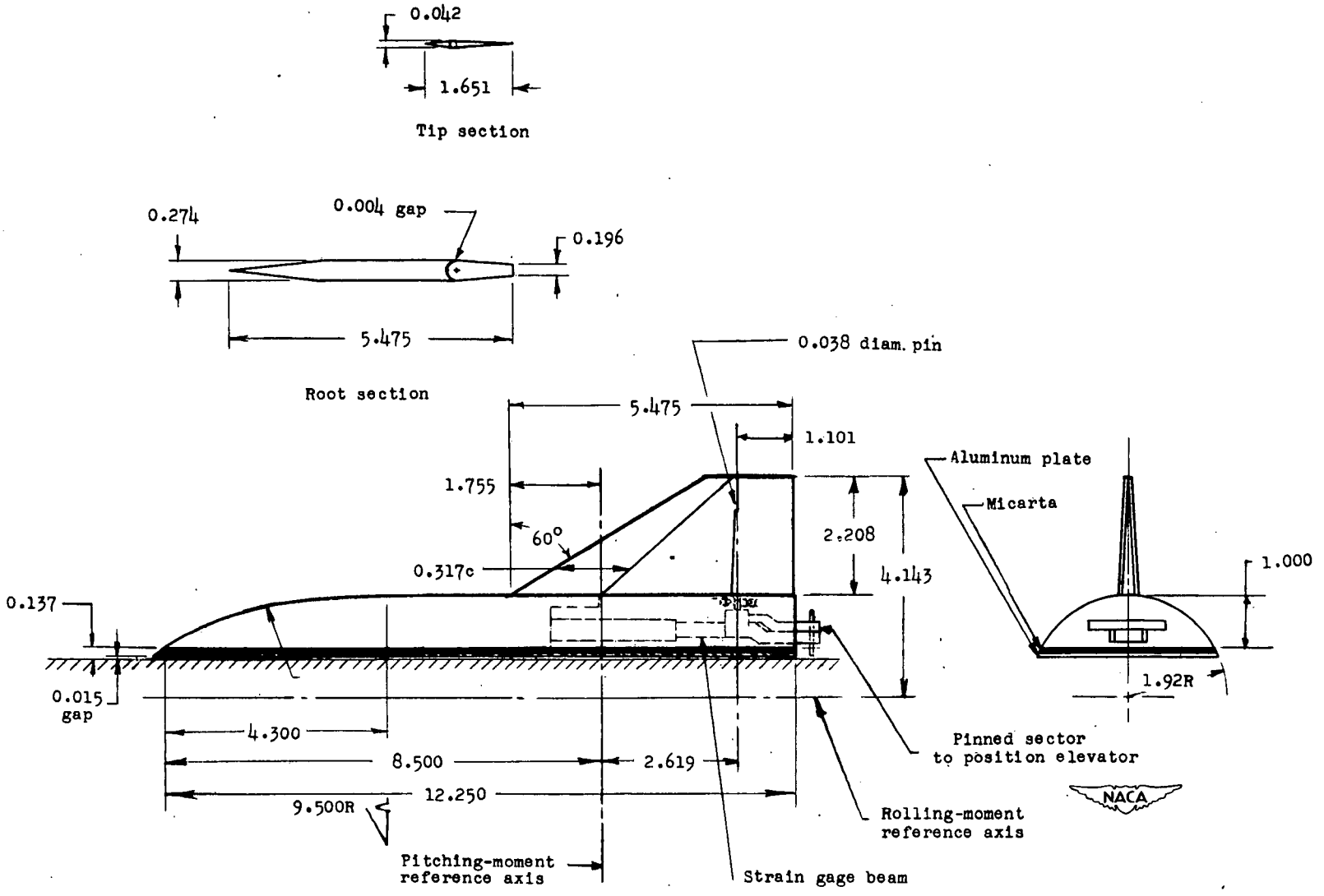

Figure 1.- Details of 0.6-scale model of Falcon (MX-904) tail surface attached to partial-span body. (All dimensions in inches.)

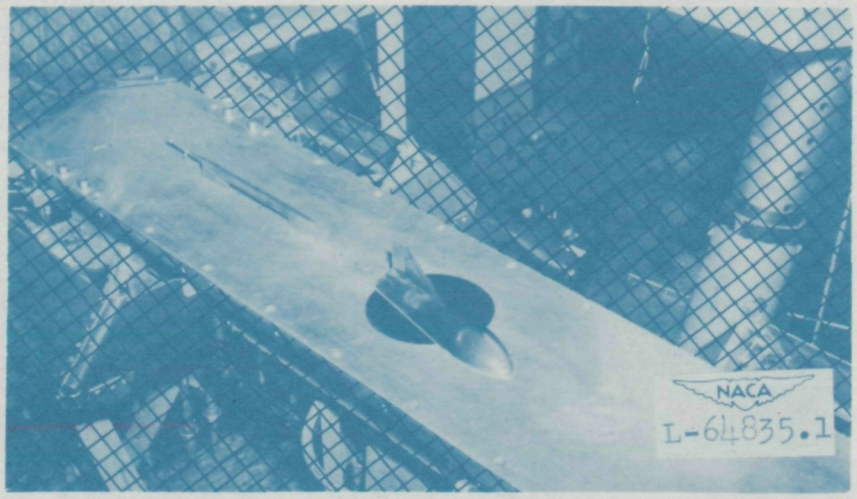

(a) Model mounted for testing in 9- by 12-inch blowdown tunnel with nozzle blocks removed.

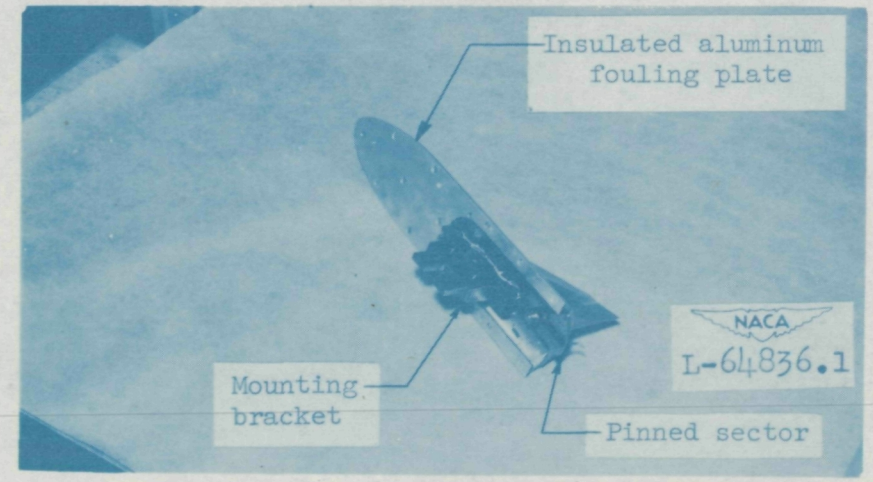

(b) Details of underside of model.

Figure 2.- Photographs of 0.6-scale partial-span model of Falcon (MX-904) missile.

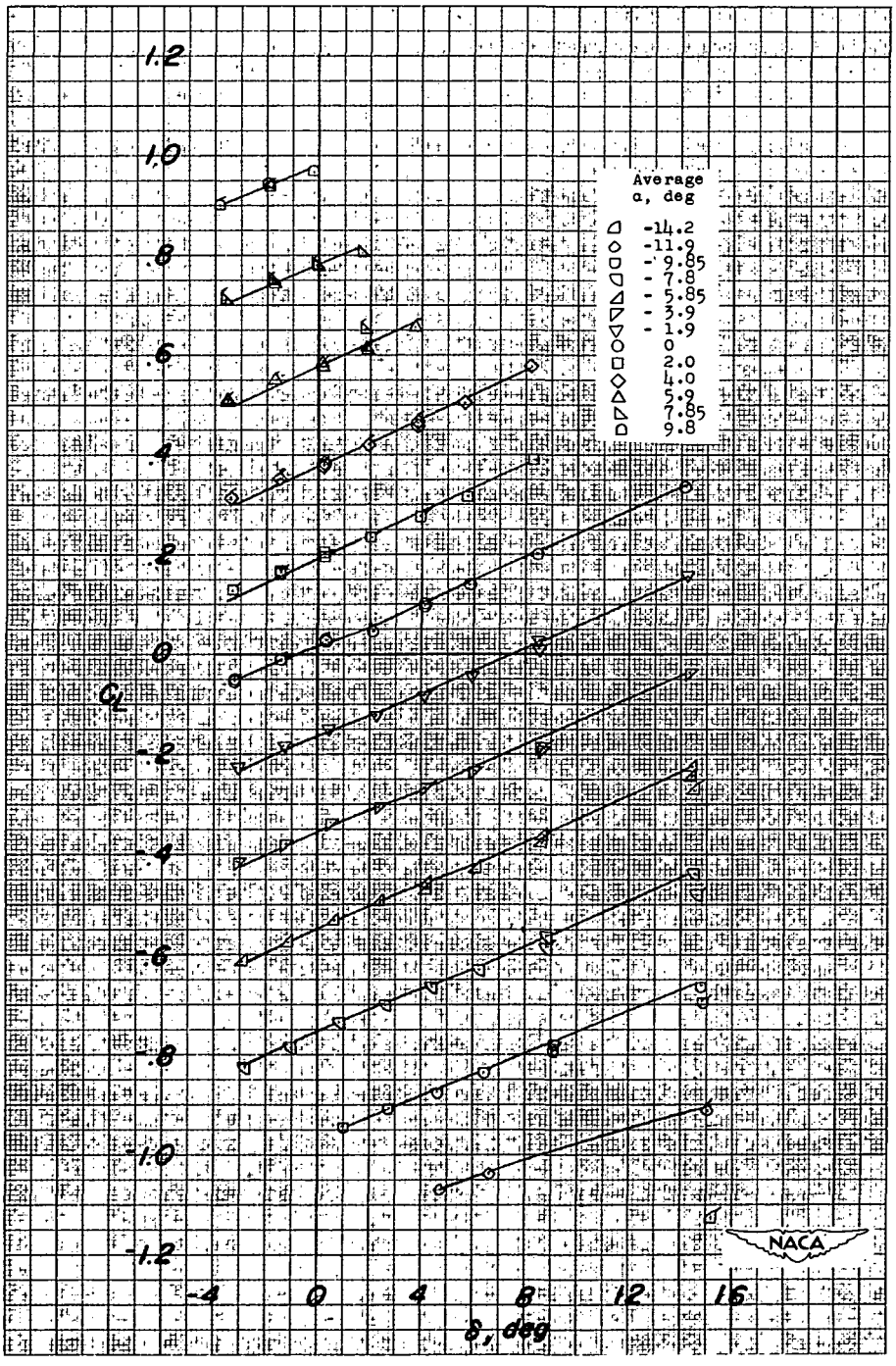

(a) Lift.

Figure 3.- Variation of aerodynamic characteristics with elevator deflection of 0.6-scale model of Falcon (MX-904) tail surface combined with partial-span body (B_2T). M = 1.62. (Flagged symbols denote check tests.)

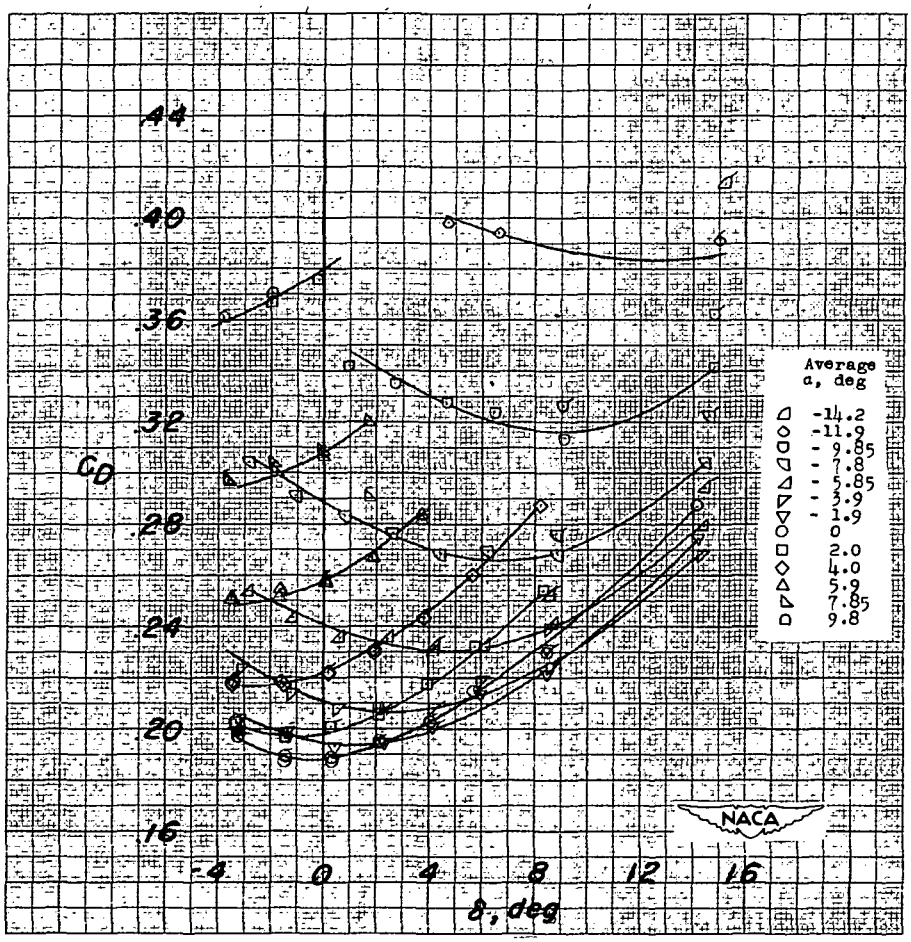

(b) Drag.

Figure 3.- Continued.

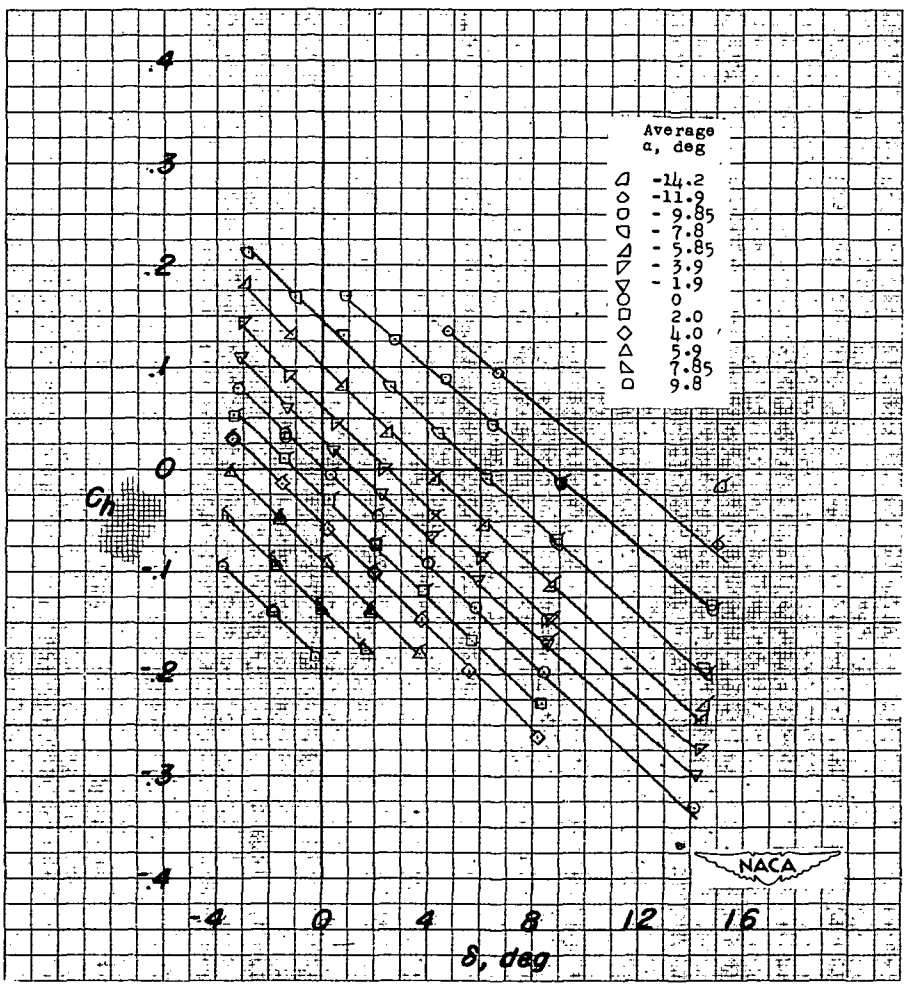

(c) Elevator hinge moment.

Figure 3.- Continued.

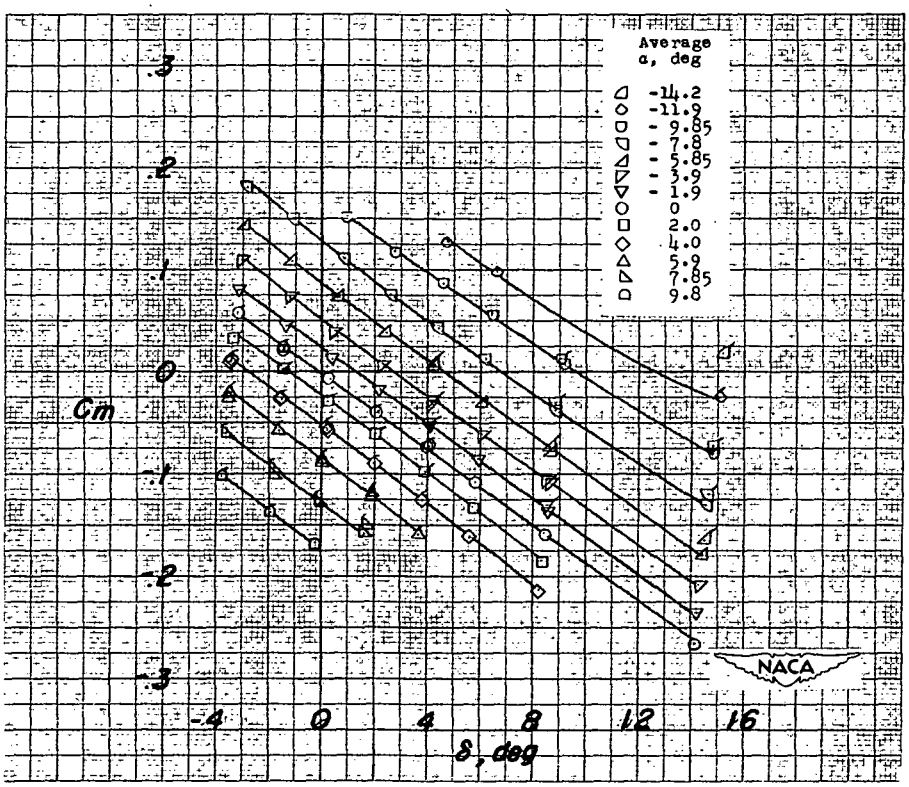

(d) Pitching moment.

Figure 3.- Continued.

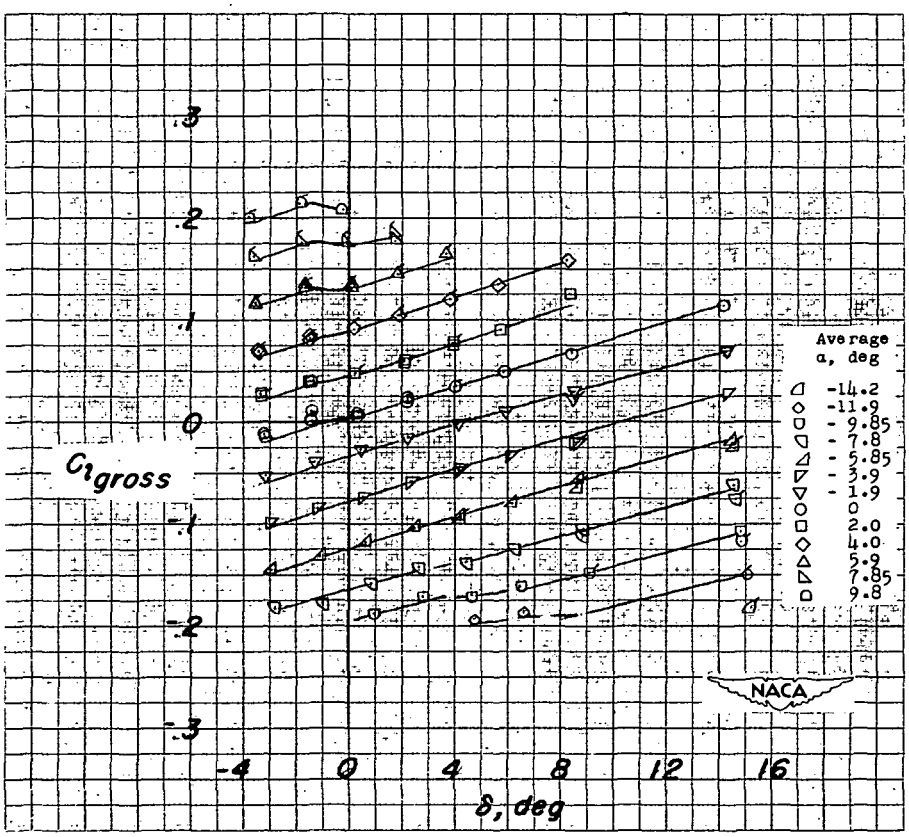

(e) Rolling moment.

Figure 3.- Continued.

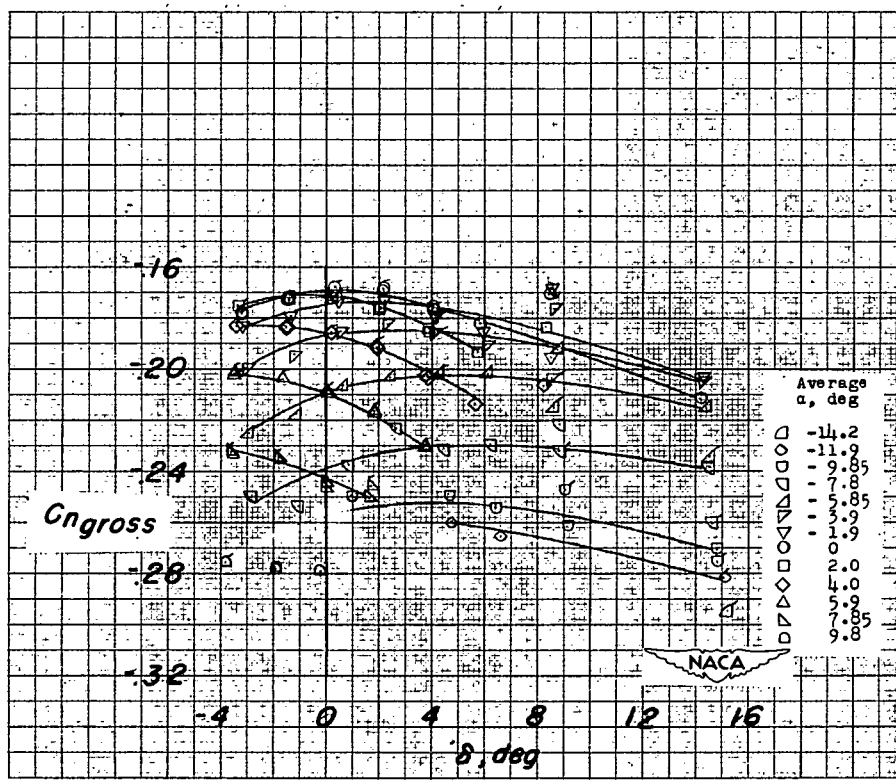

(f) Yawing moment.

Figure 3.- Concluded.

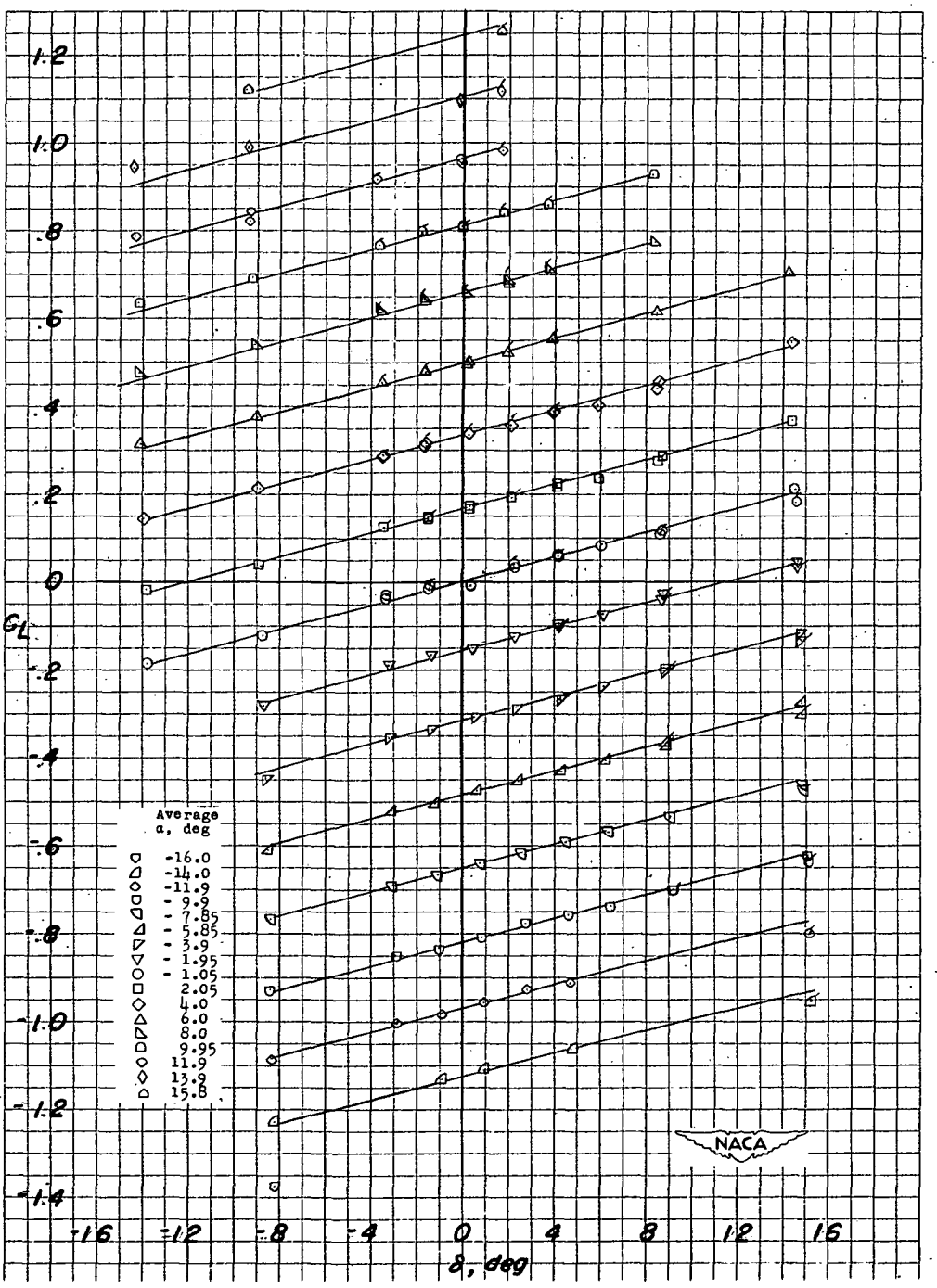

(a) Lift.

Figure 4.- Variation of aerodynamic characteristics with elevator deflection of 0.6-scale model of Falcon (MX-904) tail surface combined with partial-span body (B_2T). M = 1.96. (Flagged symbols denote check tests.)

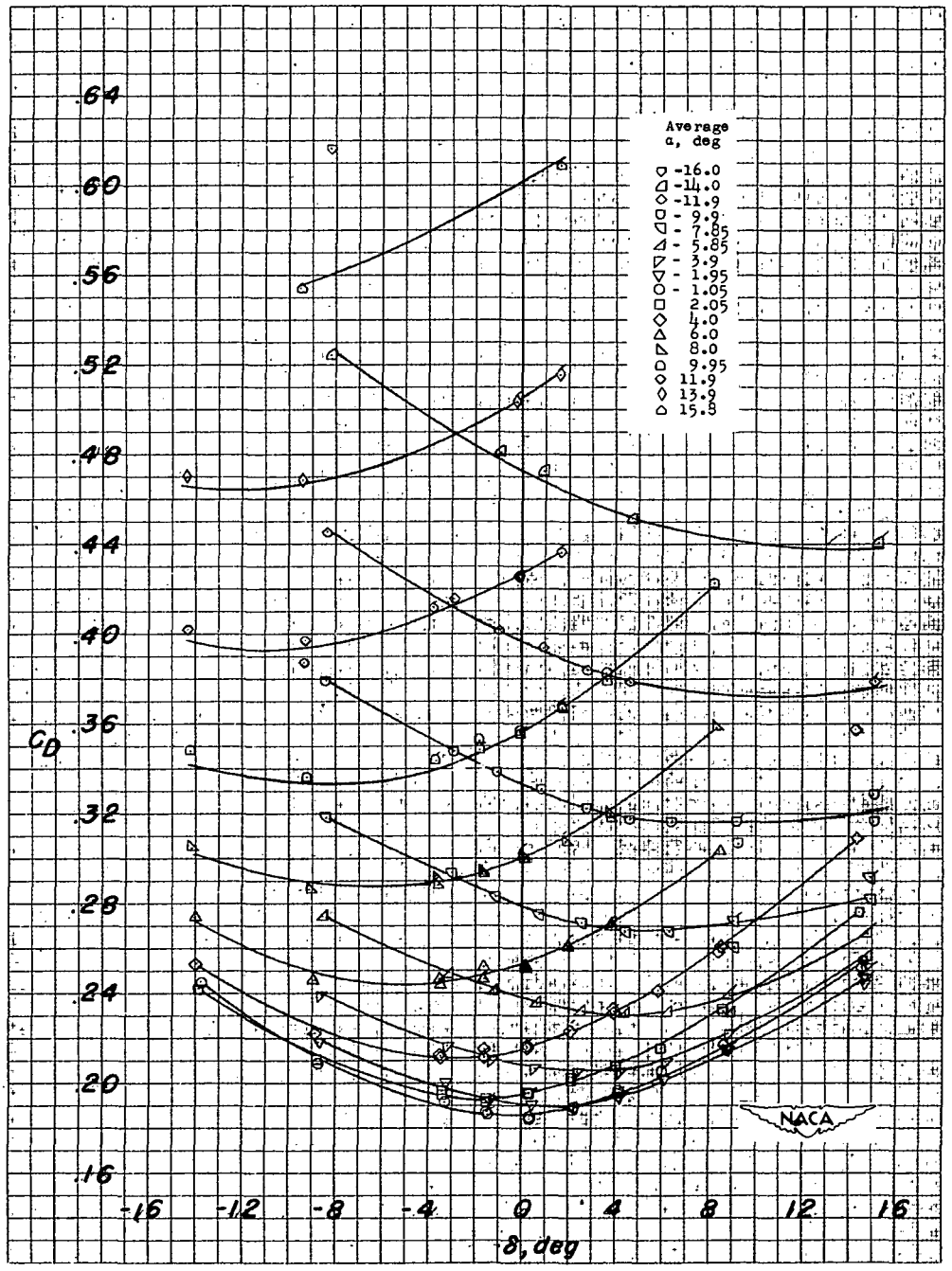

(b) Drag.

Figure 4.- Continued.

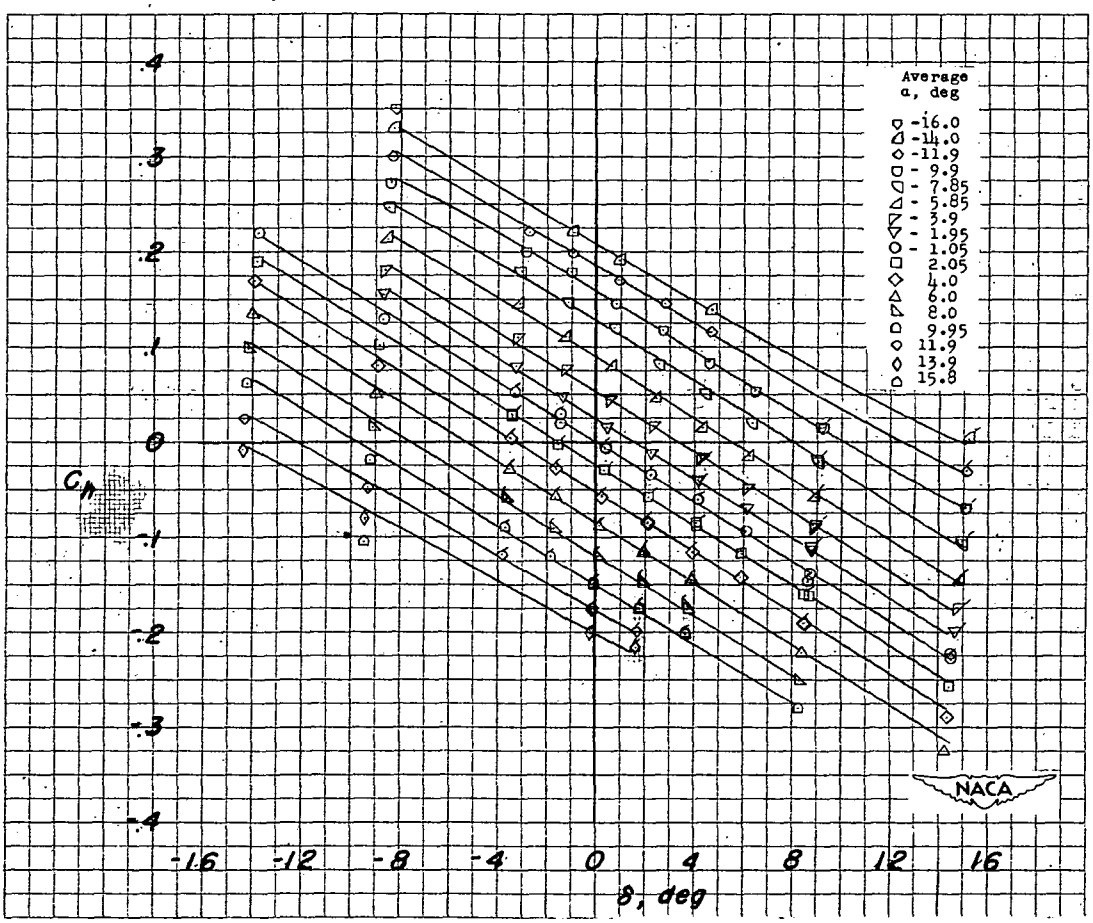

(c) Elevator hinge moment.

Figure 4.- Continued.

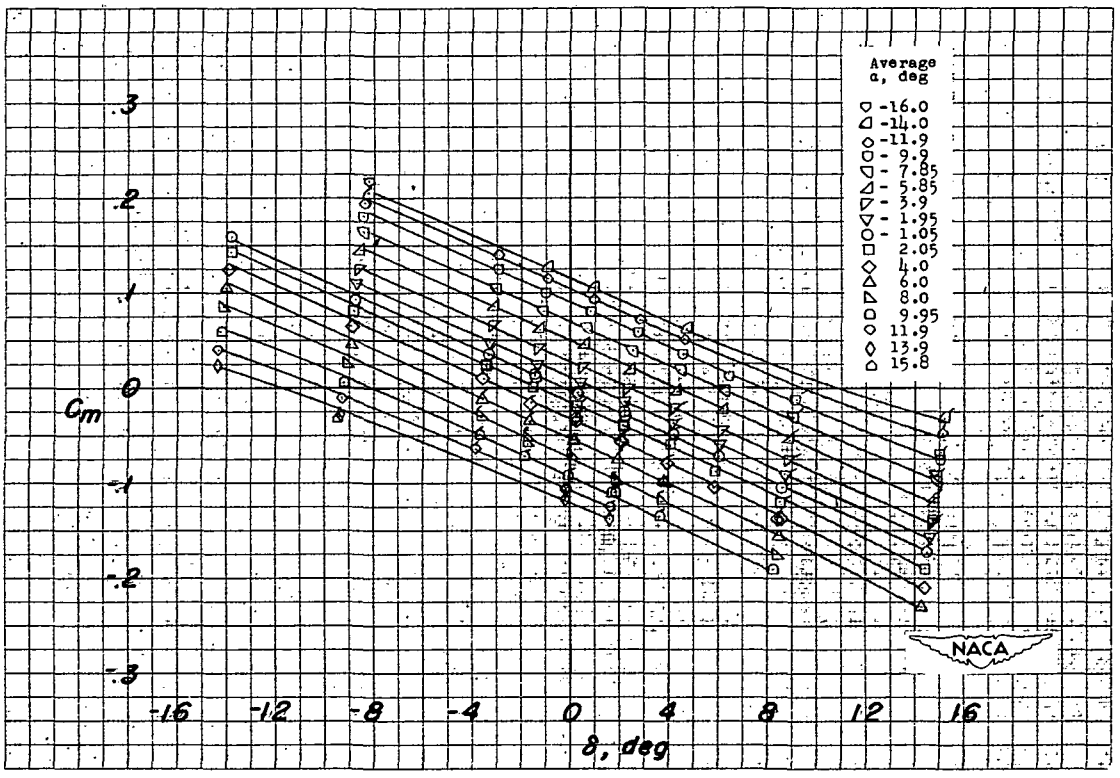

(d) Pitching moment.

Figure 4.- Continued.

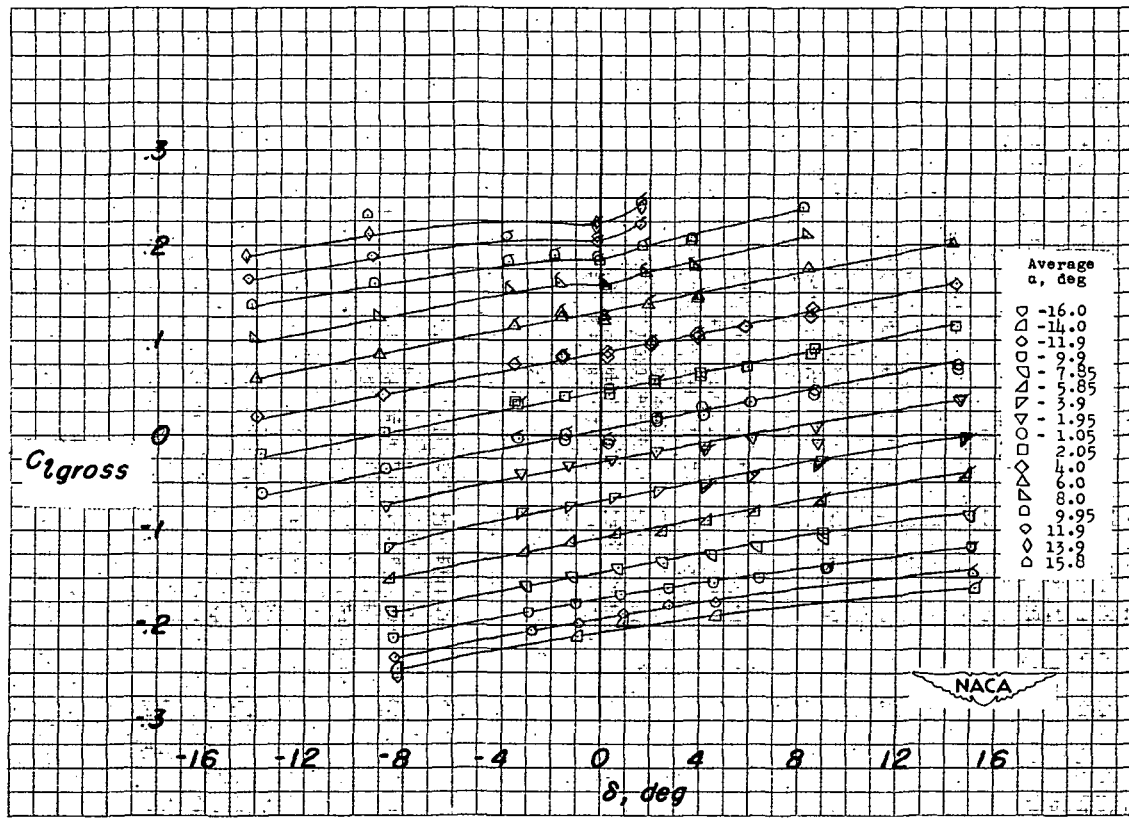

(e) Rolling moment.

Figure 4.- Continued.

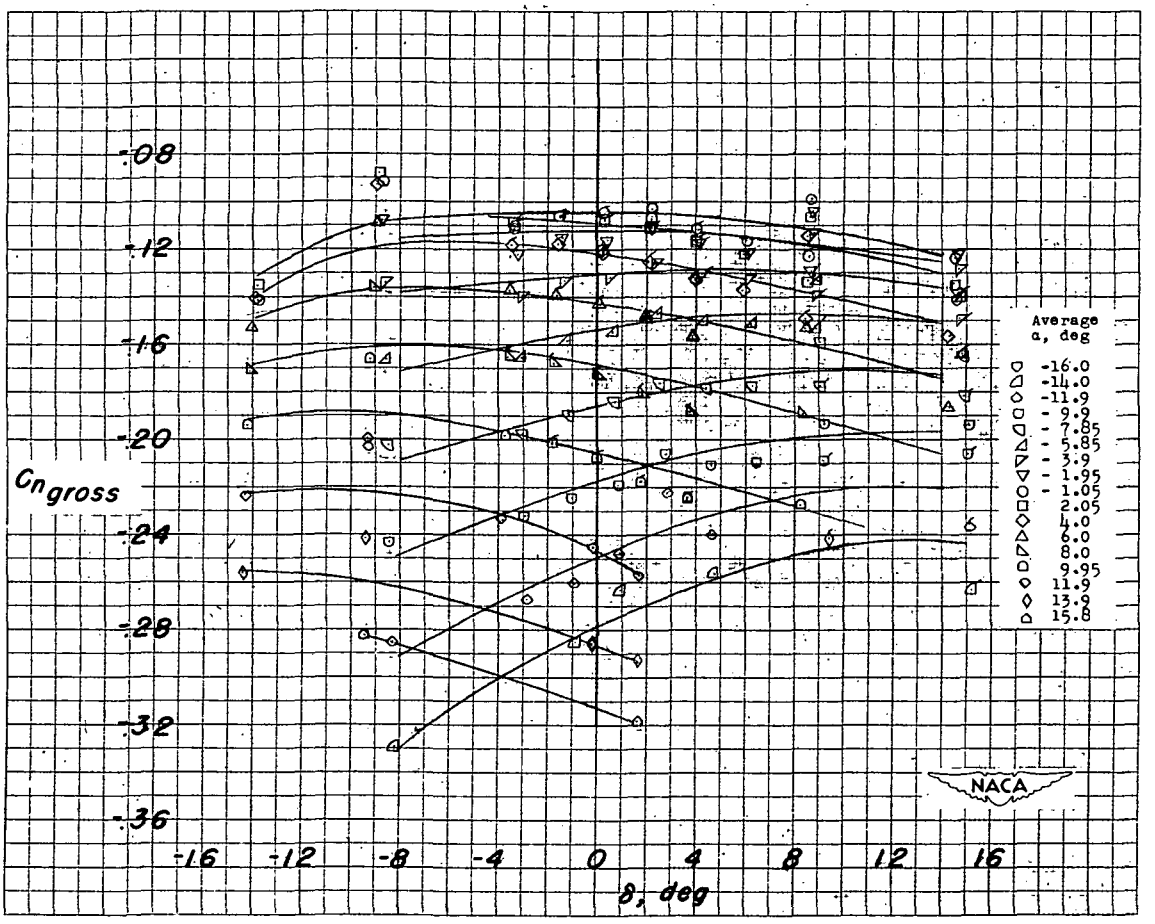

(f) Yawing-moment.

Figure 4.- Concluded.

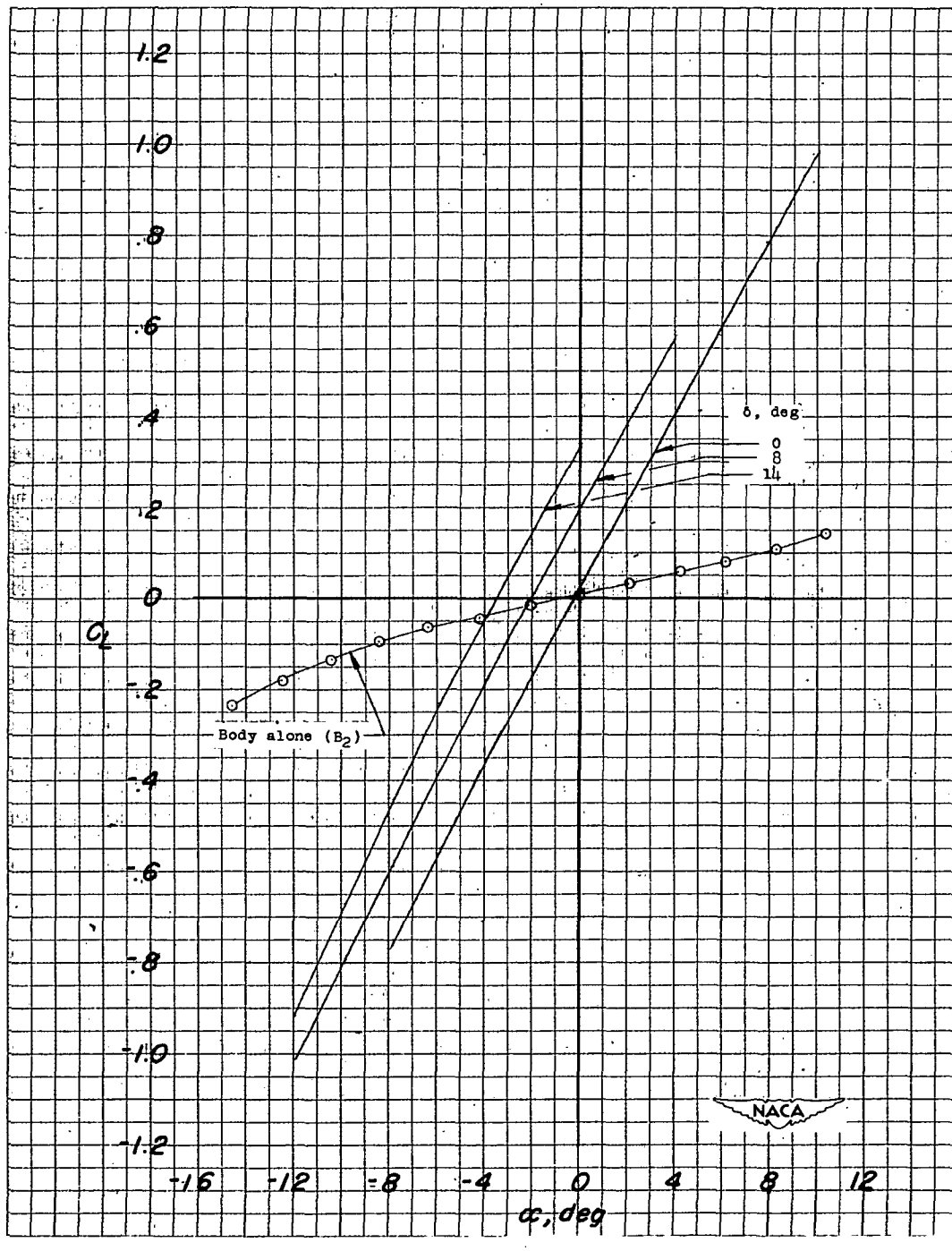

(a) Lift.

Figure 5.- Variation of aerodynamic characteristics with angle of attack of 0.6-scale model of Falcon (MX-904) tail surface combined with partial-span body (B_2T). M = 1.62.

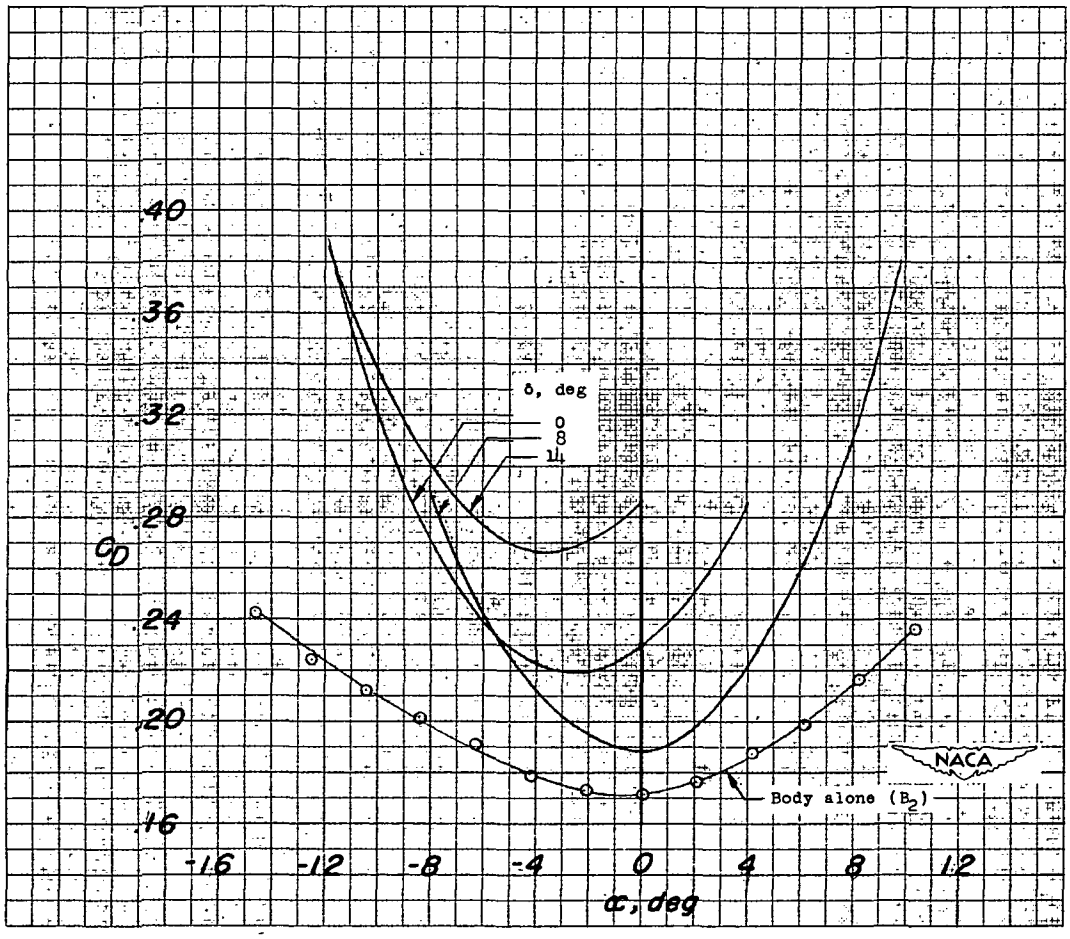

(b) Drag.

Figure 5.- Continued.

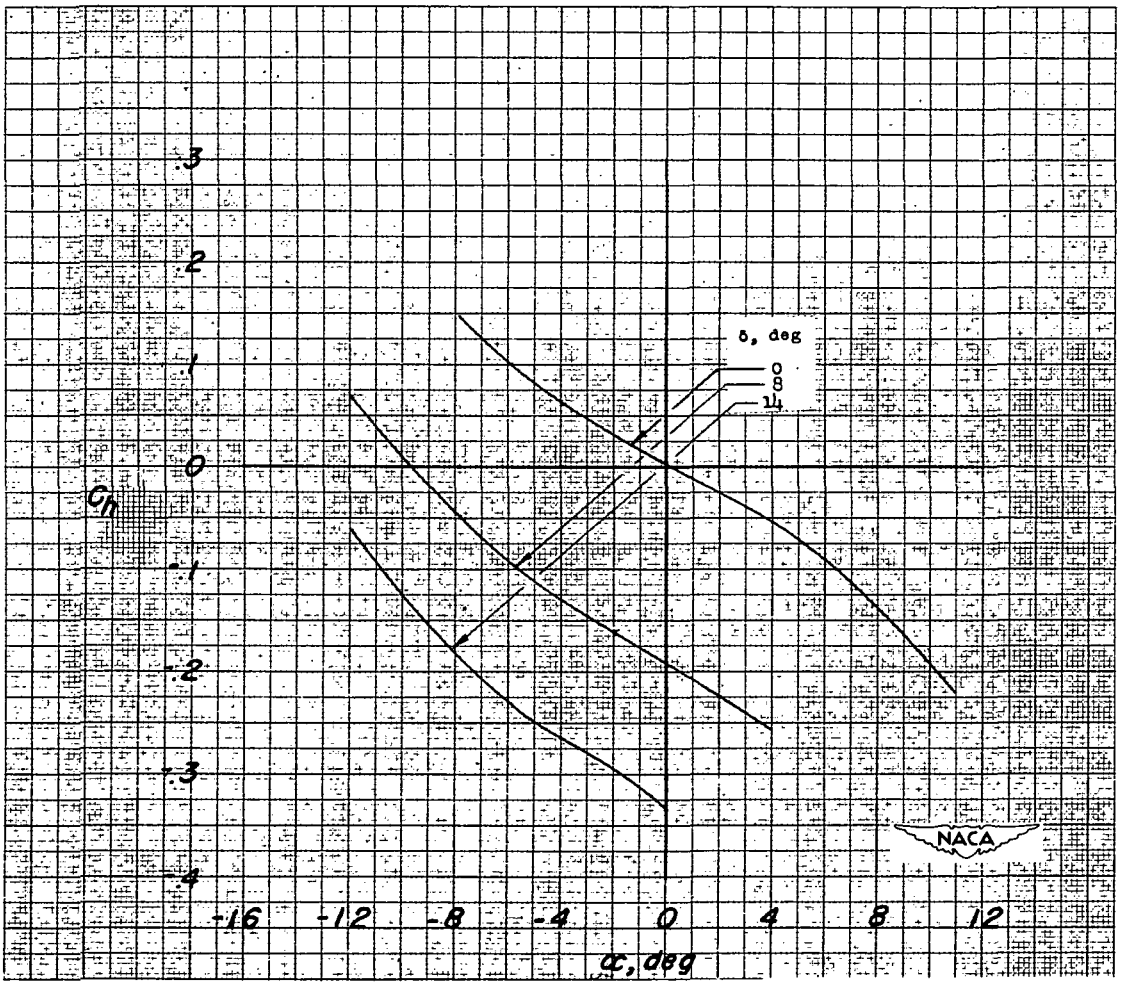

(c) Elevator hinge moment.

Figure 5.- Continued.

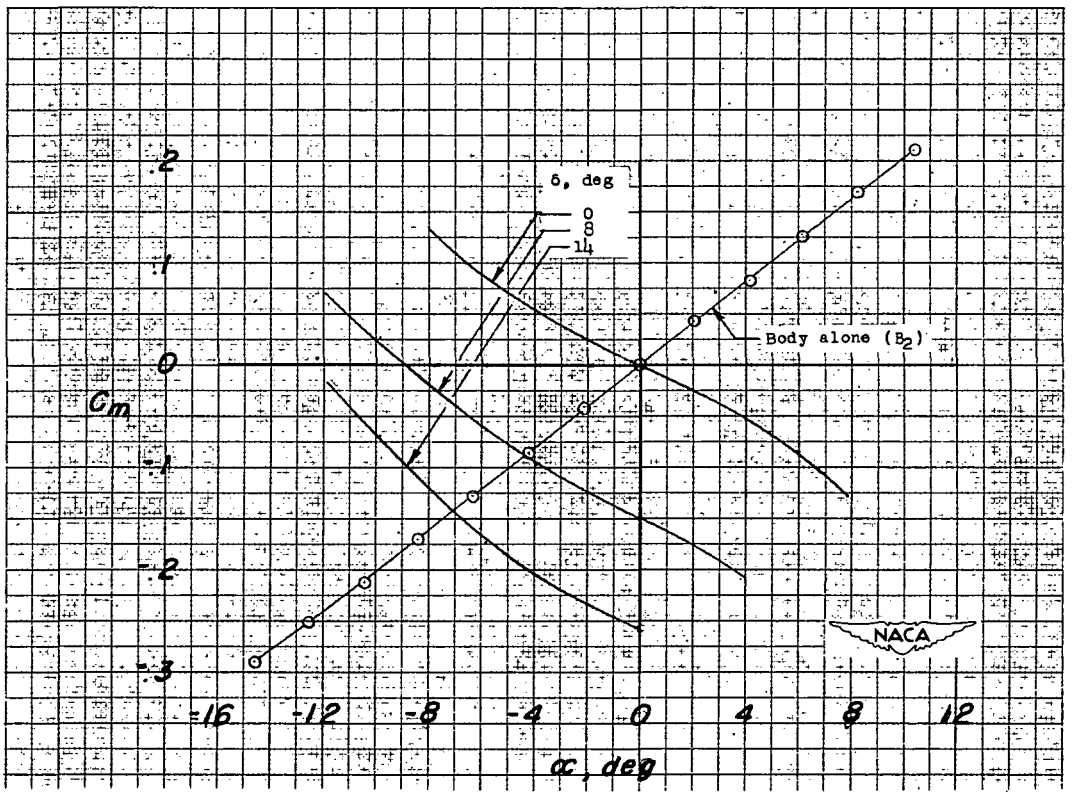

(d) Pitching moment.

Figure 5.- Continued.

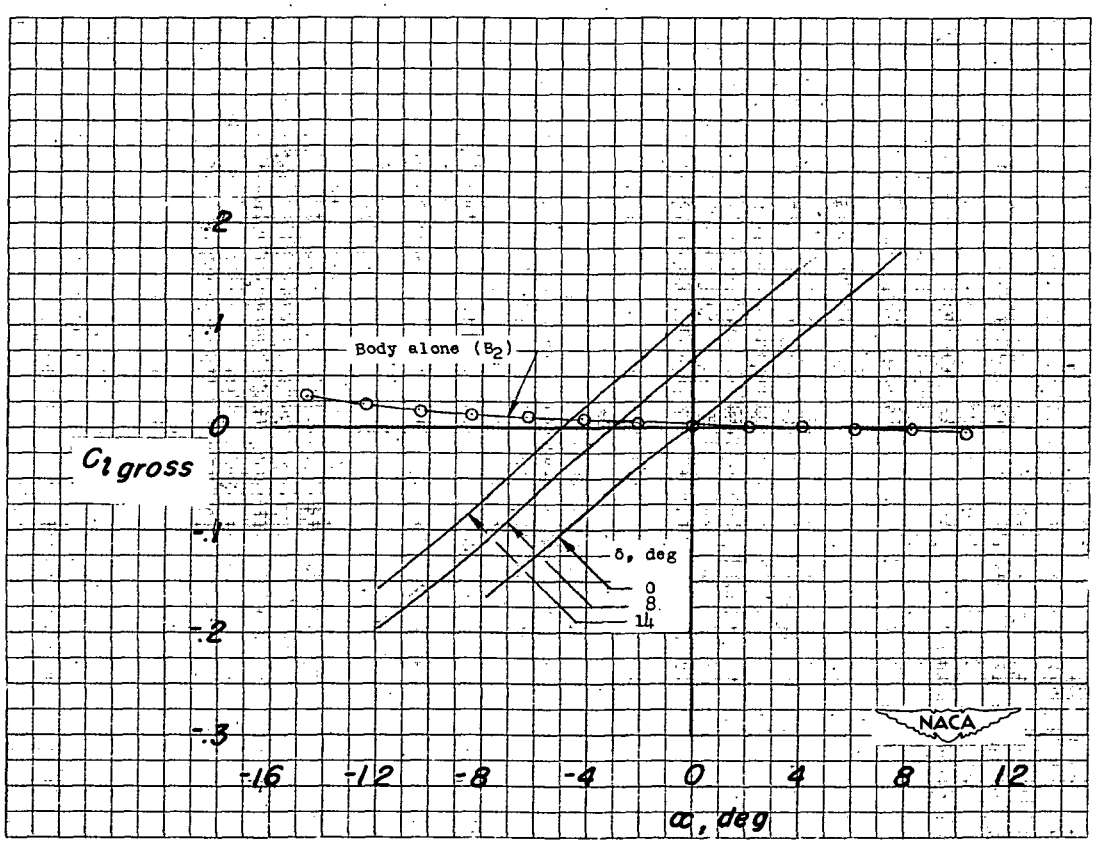

(e) Rolling moment.

Figure 5.- Continued.

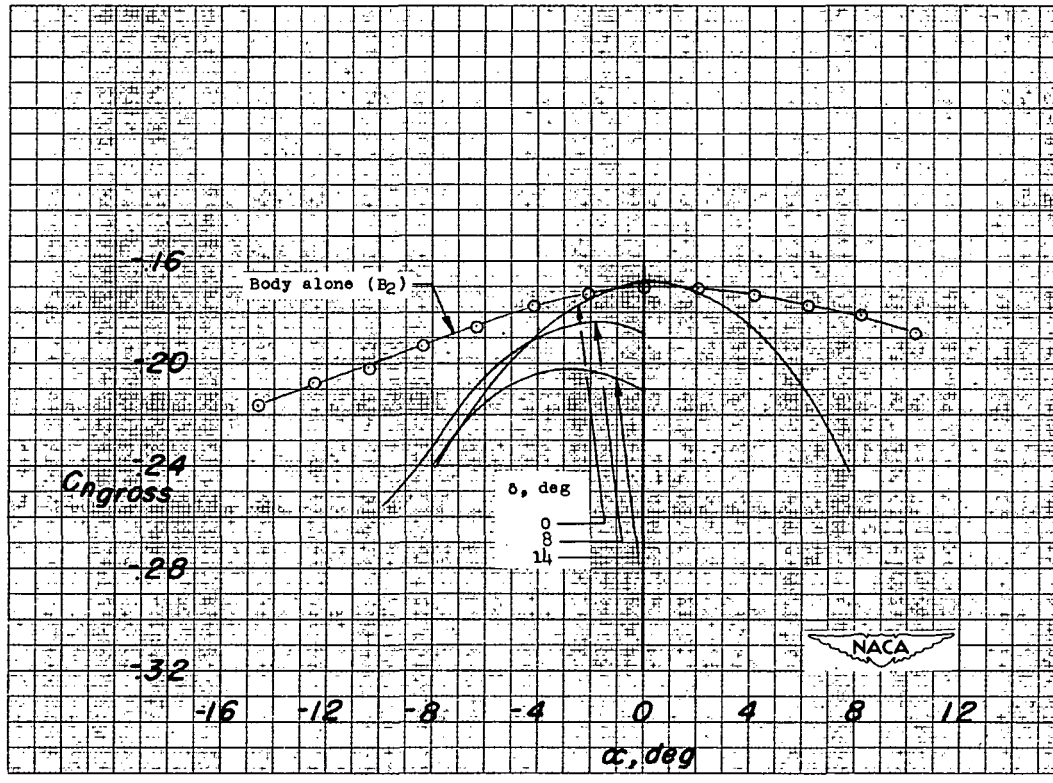

(f) Yawing moment.

Figure 5.- Concluded.

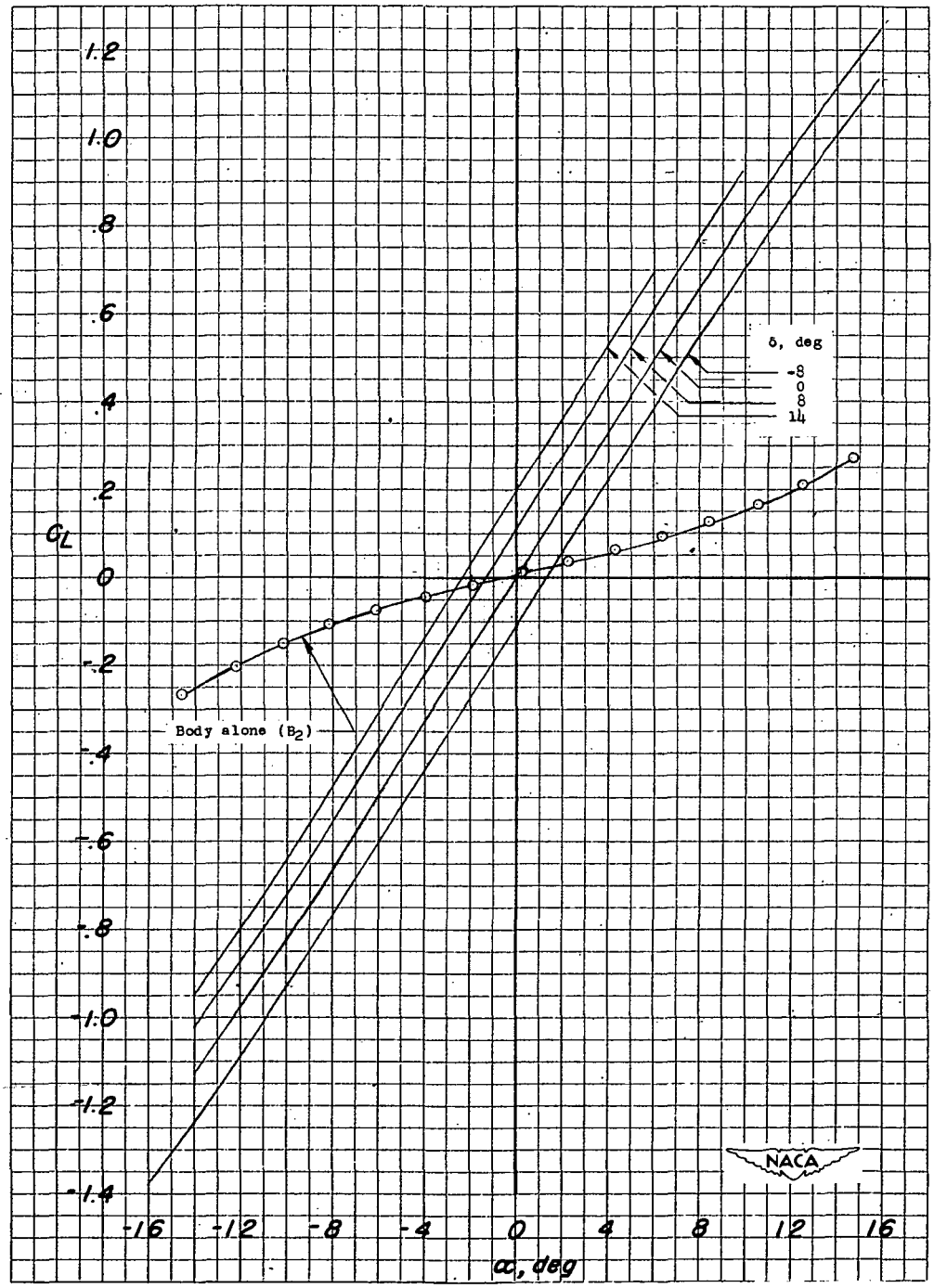

(a) Lift.

Figure 6.- Variation of aerodynamic characteristics with angle of attack of 0.6-scale model of Falcon (MX-904) tail surface combined with partial-span body (B_2T). M = 1.96.

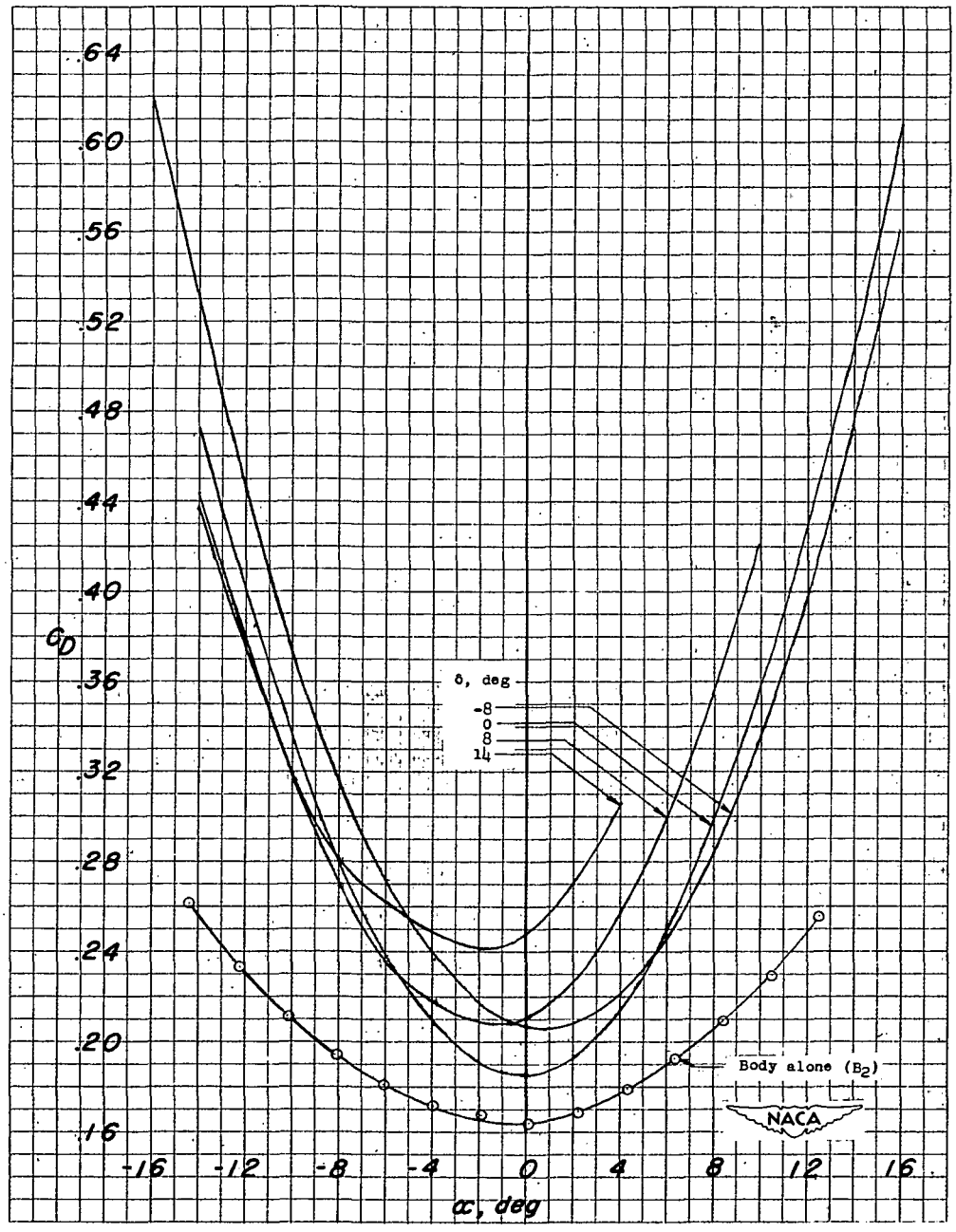

(b) Drag.

Figure 6.- Continued.

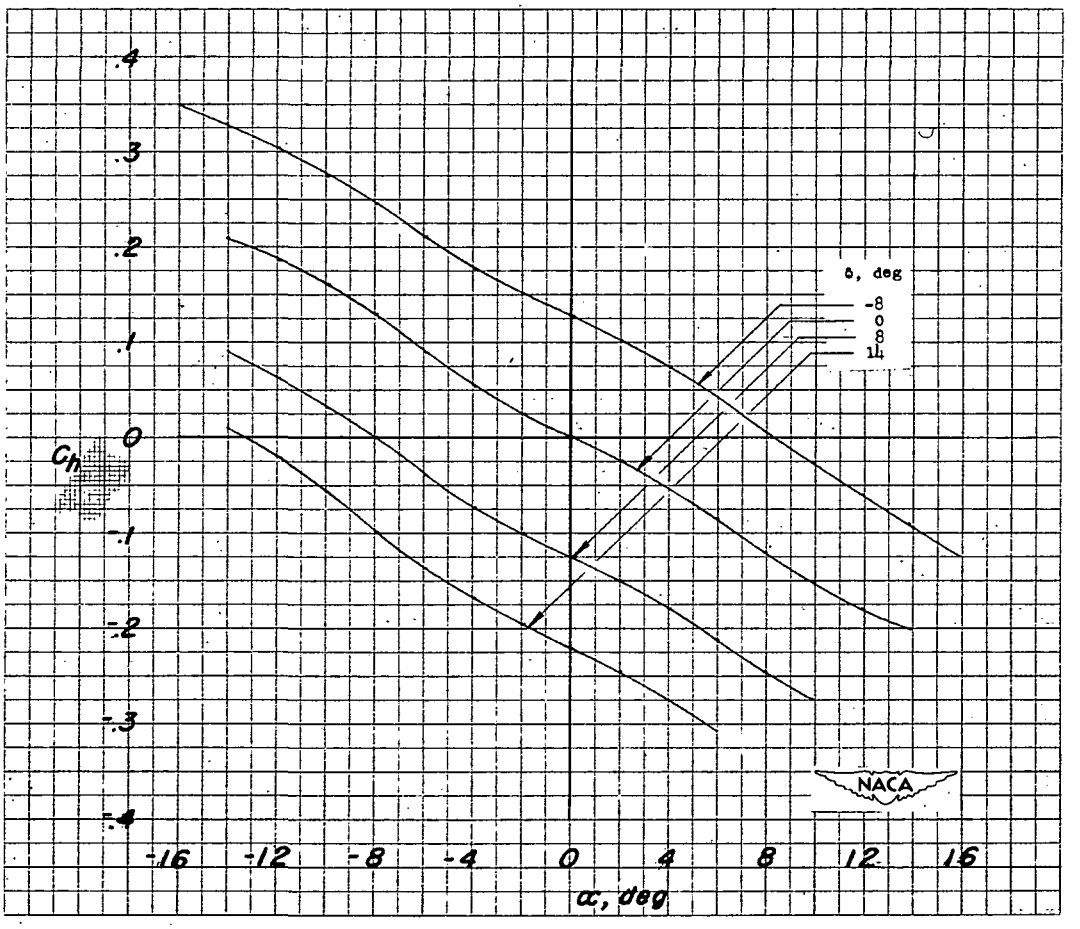

(c) Elevator hinge moment.

Figure 6.- Continued.

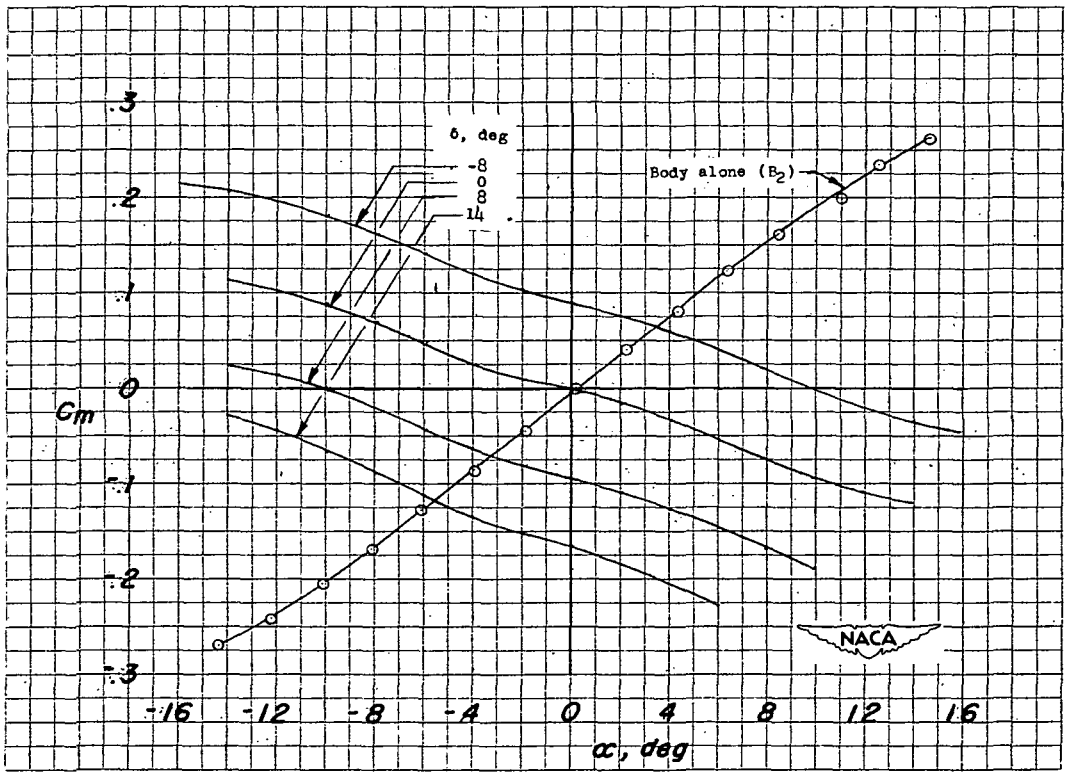

(d) Pitching moment.

Figure 6.- Continued.

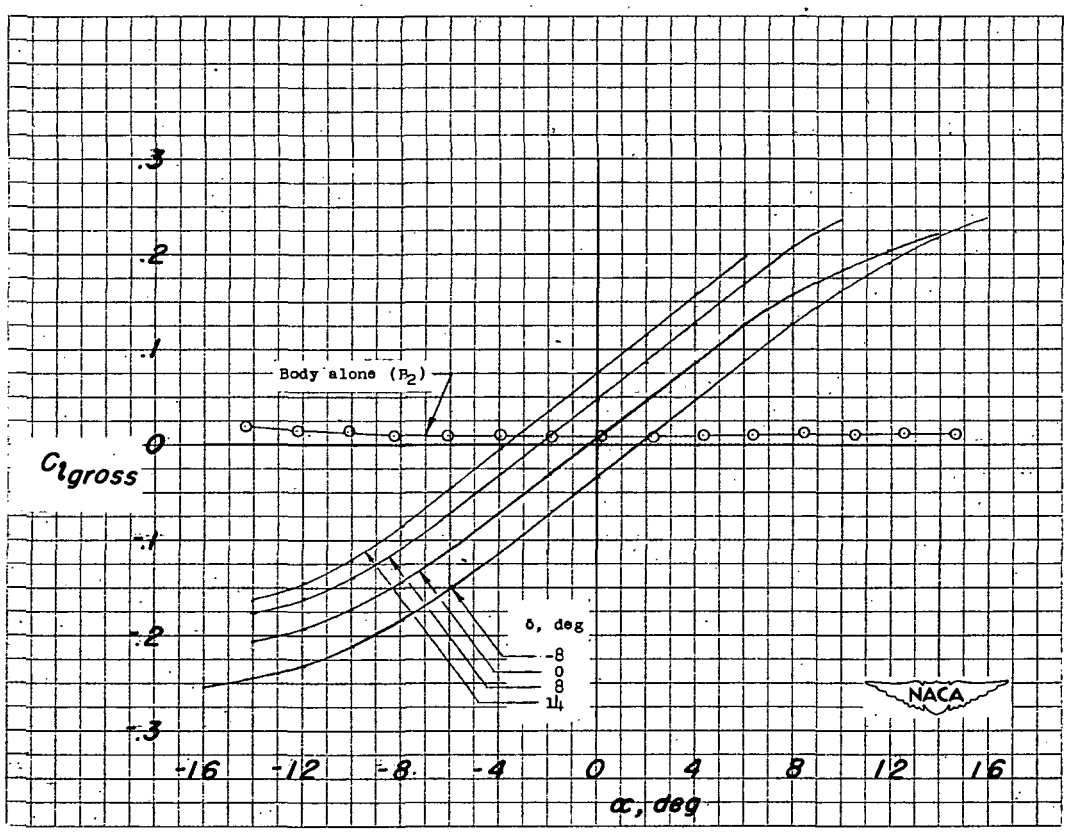

(e) Rolling moment.

Figure 6.- Continued.

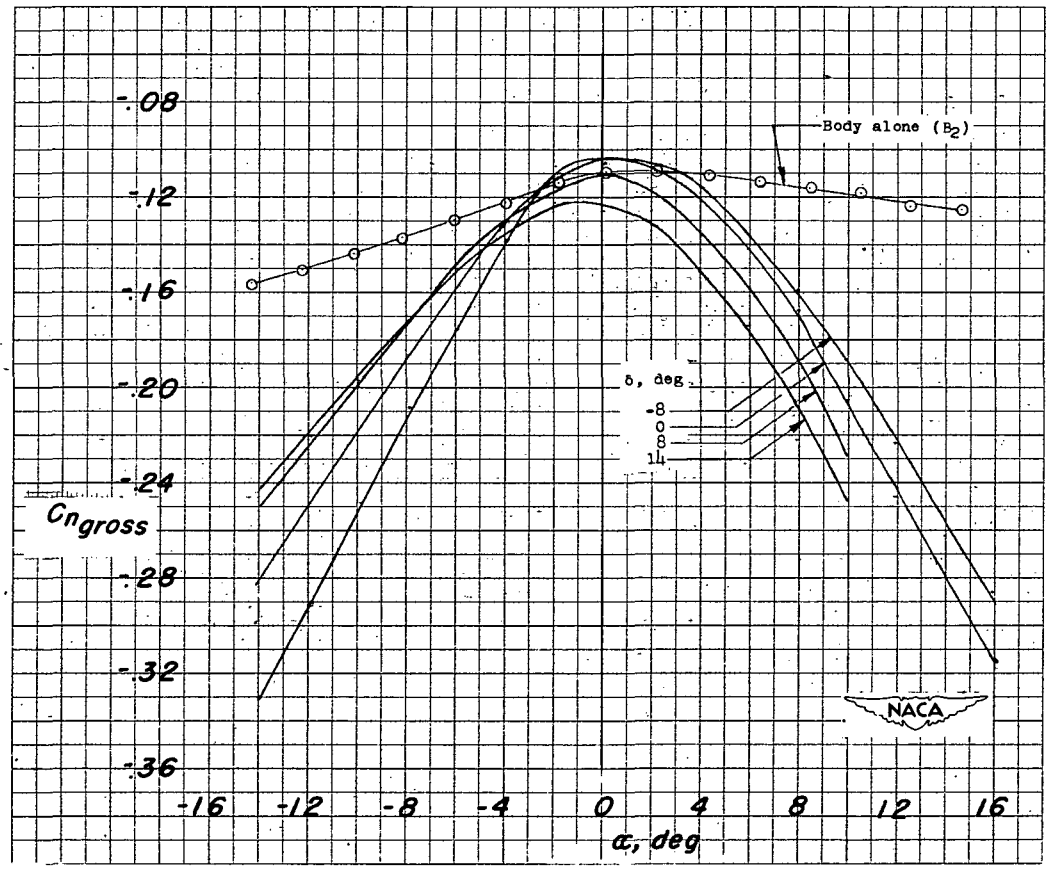

(f) Yawing moment.

Figure 6.- Concluded.

Tail-Body Combinations - Missiles 1.7.2.1.2
S

NACA

Wind-Tunnel Investigation of a 0.6-Scale Model of Hughes MX-904 Tail Surface at Supersonic Speeds. Tail Attached to a Segment of the Foreshortened Body.

By D. William Conner and Lawrence D. Guy

NACA RM SL50E10
May 1950

Missiles - Specific Types 1.7.2.2
S

NACA

Wind-Tunnel Investigation of a 0.6-Scale Model of Hughes MX-904 Tail Surface at Supersonic Speeds. Tail Attached to a Segment of the Foreshortened Body.

By D. William Conner and Lawrence D. Guy

NACA RM SL50E10
May 1950

Control - Hinge Moments 1.8.2.5
S

NACA

Wind-Tunnel Investigation of a 0.6-Scale Model of Hughes MX-904 Tail Surface at Supersonic Speeds. Tail Attached to a Segment of the Foreshortened Body.

By D. William Conner and Lawrence D. Guy

NACA RM SL50E10
May 1950

Conner, D. William, and Guy, Lawrence D.
S

NACA

Wind-Tunnel Investigation of a 0.6-Scale Model of Hughes MX-904 Tail Surface at Supersonic Speeds. Tail Attached to a Segment of the Foreshortened Body.

By D. William Conner and Lawrence D. Guy

NACA RM SL50E10
May 1950